Biomech Model Mechanobiol (2017) 16:5–14
DOI 10.1007/s10237-016-0798-x

ORIGINAL PAPER

Computational simulation of bone fracture healing under inverse dynamisation

Cameron J. Wilson[1,2] · **Michael A. Schütz**[1,3] · **Devakara R. Epari**[1]

Received: 15 October 2015 / Accepted: 9 May 2016 / Published online: 24 May 2016

Abstract Adaptive finite element models have allowed researchers to test hypothetical relationships between the local mechanical environment and the healing of bone fractures. However, their predictive power has not yet been demonstrated by testing hypotheses ahead of experimental testing. In this study, an established mechano-biological scheme was used in an iterative finite element simulation of sheep tibial osteotomy healing under a hypothetical fixation regime, "inverse dynamisation". Tissue distributions, interfragmentary movement and stiffness across the fracture site were compared between stiff and flexible fixation conditions and scenarios in which fixation stiffness was increased at a discrete time-point. The modelling work was conducted blind to the experimental study to be published subsequently. The simulations predicted the fastest and most direct healing under constant stiff fixation, and the slowest healing under flexible fixation. Although low fixation stiffness promoted more callus formation prior to bridging, this conferred little additional stiffness to the fracture in the first 5 weeks. Thus, while switching to stiffer fixation facilitated rapid subsequent bridging of the fracture, no advantage of inverse dynamisation could be demonstrated. In vivo data remains necessary to conclusively test this treatment protocol and this will, in turn, provide an evaluation of the model's performance. The publication of both hypotheses and their computational simulation, prior to experimental testing, offers an appealing means to test the predictive power of mechano-biological models.

Keywords Fracture healing · Fracture fixation · Models · Biological · Dynamisation

1 Introduction

The healing of diaphyseal bone fractures is strongly influenced by the mechanical environment, which is in turn dependent on the bone and fracture geometry and applied loads, displacements and fixation. As reviewed in detail elsewhere (Doblaré et al. 2004; Geris et al. 2009; Isaksson 2012; Khayyeri et al. 2013; Pivonka and Dunstan 2012), a number of conceptual models have been developed, linking local mechanical conditions to tissue formation, transformation and removal processes throughout secondary bone healing (i.e. healing via formation of a temporary callus). Finite element models based on published experimental data have enabled researchers to quantify these conceptual relationships (Pivonka and Dunstan 2012). Over the past 15 years, the development of iterative, adaptive models has allowed testing of the models' ability to predict the succession of healing observed experimentally—in particular, the distribution of tissues in the callus and fracture site and the restoration of mechanical integrity over time. Computational models of fracture healing mechanobiology may be an effective tool for

Electronic supplementary material The online version of this article (doi:10.1007/s10237-016-0798-x) contains supplementary material, which is available to authorized users.

✉ Devakara R. Epari
d.epari@qut.edu.au

[1] Institute of Health and Biomedical Innovation, Queensland University of Technology (QUT), GPO Box 2434, Brisbane, QLD 4001, Australia

[2] Brisbane Hip Clinic, Suite 7-2, St Andrew's Specialist Centre, St Andrew's War Memorial Hospital, 457 Wickham Tce, Spring Hill, QLD 4000, Australia

[3] Trauma Service, Princess Alexandra Hospital, Ipswich Road, Woolloongabba, QLD 4102, Australia

hypothesis testing and treatment optimisation (Pivonka and Dunstan 2012). However, to date, their use in testing specific hypotheses ahead of experimental testing has not been reported.

Mechano-biological simulations may be broadly classified by the parameters used to regulate biological changes—in this case, the growth and differentiation of callus tissues. The most common are fluid flow and shear strain, for poroelastic formulations (Andreykiv et al. 2008; Byrne et al. 2011; Checa et al. 2011; Geris et al. 2010; González-Torres et al. 2010; Hayward and Morgan 2009; Isaksson et al. 2008, 2009; Kuiper et al. 2000; Lacroix and Prendergast 2002a, b; Lacroix et al. 2002), many based on the scheme of Prendergast et al. (Huiskes et al. 1997; Prendergast and Huiskes 1996; Prendergast et al. 1997; van Driel et al. 1998), and deviatoric and dilatational stresses and/or strains, for elastic formulations (Bailón-Plaza and van der Meulen 2003; Chen et al. 2009; Shefelbine et al. 2005; Simon et al. 2011; Steiner et al. 2013, 2014a, b; Wehner et al. 2010, 2012, 2014), based primarily on the concept of Claes and Heigele (1999). Principal strains have also been used (Witt et al. 2011), and other models have used a single parameter to quantify the mechanical environment in a general way (Ament and Hofer 2000; García-Aznar et al. 2007; Gómez-Benito et al. 2005, 2006; Vetter et al. 2012). In addition to mechanical regulation, the iterative models have required the addition of a biological component—cell populations, growth factors, vascularity and/or a composite "biological potential"—in order to adequately replicate the temporal and spatial development of the callus (Andreykiv et al. 2008; Bailón-Plaza and van der Meulen 2003; Checa et al. 2011; Chen et al. 2009; Geris et al. 2010; Gómez-Benito et al. 2005; Isaksson et al. 2008; Lacroix et al. 2002; Repp et al. 2015; Shefelbine et al. 2005; Simon et al. 2011; Vetter et al. 2012). The simulations achieve broad agreement with the generalised progression of secondary bone healing, as presented by e.g. Einhorn (1998) and McKibbin (1978). Each scheme produces broadly similar simulations: this may be attributed in part to models typically being regulated by a volumetric and a distortional mechanical parameter (Isaksson et al. 2006a, b). It also likely corresponds to the phenomenological nature of most of the models (Geris et al. 2009), in which quantitative relationships between tissue changes and mechanical parameters are based on similar or identical experimental data.

Generally, the simulations predict that low mechanical stimuli—reduced loading, small fracture gaps, increased fixation stiffness, and low interfragmentary strain—produce the fastest healing (Chen et al. 2009; García-Aznar et al. 2007; Geris et al. 2010; Gómez-Benito et al. 2005, 2006; Isaksson et al. 2008; Kuiper et al. 2000; Lacroix and Prendergast 2002a, b; Simon et al. 2011; Wehner et al. 2010, 2012, 2014). Moderately low mechanical stimuli tend to favour bone formation, while higher stimuli favour cartilage and fibrous tissue production, particularly in early stages of healing (González-Torres et al. 2010; Lacroix and Prendergast 2002a; Simon et al. 2011), or delay endochondral ossification in later stages (Isaksson et al. 2008). The assessment of models' performance in predicting the spatial and temporal development of tissues in the callus is made difficult, though, by the limited experimental data available. Therefore, many of the models have been evaluated against general trends or mechanical (e.g., stiffness) or temporal (e.g., time to bridging) data.

Thorough validation requires simulations to be compared with data other than those used in tuning the models (Isaksson et al. 2006a). This form of validation has been a relatively recent development in bone healing models (Chen et al. 2009; Hayward and Morgan 2009; Isaksson et al. 2006a; Steiner et al. 2013, 2014a), but it remains limited with respect to histological comparisons. These are a critical component in assessing whether tissue growth and differentiation criteria are functioning correctly. Only a small number of experimental studies (Claes and Heigele 1999; Epari et al. 2006; Peters et al. 2010; Vetter et al. 2010) have been published with both the well defined mechanical conditions and the histological data at multiple time-points needed for thorough validation. Due to practical limitations, most studies present only end-point histology, which allows little insight into the progression that led to it. Polychrome labelling (Claes and Heigele 1999; Claes et al. 2000; Stürmer 1984) addresses this to some extent, by revealing bone deposition over discrete time periods. Vetter et al. (2010) sought to address this limitation in validation data, by mapping tissue distributions averaged over multiple histological samples.

An ideal test of models' predictive capacity is to simulate specific hypotheses prior to experimental testing of the same. The trends identified by models thus far tend to reflect only what is known already from in vivo studies. A small number of computational studies have predicted improved healing under specific conditions (Steiner et al. 2014b; Wehner et al. 2010, 2012, 2014), but these findings have not yet been tested experimentally. While Gómez-Benito et al. (2011) based the mechanical stimulus in their experiments on optimal parameters from a computational study (González-Torres et al. 2010), the theoretical relationship between healing and different stimulation frequencies was not experimentally confirmed. The application of models to testing hypotheses and predicting the effects of injury and treatment parameters thus remains largely unexplored.

"Inverse dynamisation" was recently proposed as a new fixation strategy (Epari et al. 2013). Its bases are that (a) flexible fixation during the early stages of healing will promote the formation of a larger callus, providing a greater effective stiffness than would result under more rigid fixation, and (b) increasing fixation stiffness after this initial callus

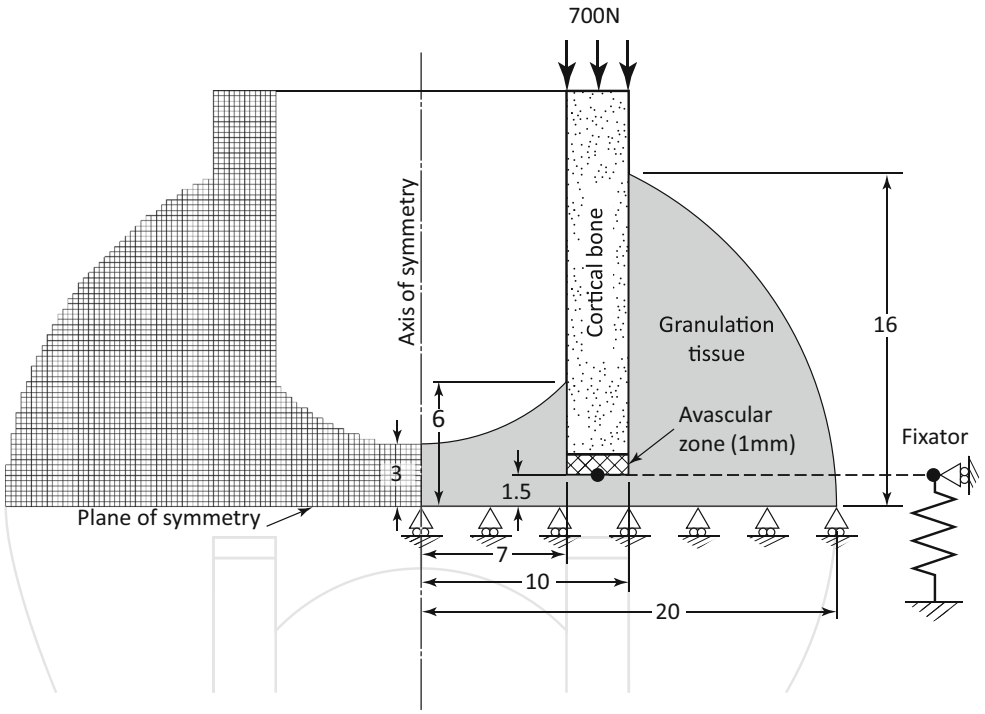

Fig. 1 Geometry, loading, boundary conditions and finite element mesh of the sheep tibial fracture model in its initial state. Symmetry is assumed about the bone axis and the mid-plane of the fracture. The fixator is represented by a spring fixed at one end and rigidly connected to the bone at the fracture edge. Interfragmentary movement is measured at this connection point

growth will facilitate rapid endochondral ossification. It is proposed that this may produce faster or comparable healing relative to an optimally stiff constant fixation, as well as offering an increased safety factor against potentially disruptive transient loads during the consolidation phase. The inverse dynamisation hypothesis has not yet been tested either experimentally or computationally. This presents an opportunity to test mechano-biological models' predictive capabilities while blinded to in vivo experimental results. This eliminates the possibility of tuning model parameters or algorithms to match specific data and thus, provides an additional level of validation that has been missing to date.

The chief aim of this study was to computationally test the hypothesis that bone healing will be faster when fixation stiffness is initially low, and increased after callus formation, than under constant fixation stiffness. The effects of the time-point at which stiffness is increased was also of interest. A published iterative mechano-biological scheme (Simon et al. 2011) was emulated, to predict the course of fracture healing under high and low fixation stiffness, and the effect of changing from flexible to stiff fixation at distinct time-points. These stand-alone predictions will be subsequently compared with the results of animal experiments.

2 Methods

An axisymmetric finite element model of a sheep tibia with a 3-mm mid-diaphyseal osteotomy was created, using four-node quadrilateral elements with a uniform 0.25-mm node spacing (Fig. 1). The bone and callus geometry was based on those presented by Lacroix et al. (2002) and Claes and Heigele (1999), with the callus shape scaled to match the larger dimensions of the tibia, compared to the metatarsal models of the Ulm group (Claes and Heigele 1999; Simon et al. 2011). The fractured bone was assumed to be symmetrical about the middle of the fracture gap. Linear elastic material properties were used, as per Simon et al. (2011) and related models.

An axial load of 700 N (Lacroix and Prendergast 2002a) was applied to the fractured face of the cortical bone, as shown by Steiner et al. (2014a). A fixator was represented by a spring between this face and the "ground" (equating to a defined stiffness between the cortical bone and the fixed plane of symmetry). Two stiffness levels were used: 6250 and 690 N/mm, restraining interfragmentary movement (IFM) to 0.1 mm (7 %) and 0.5 mm (33 %) respectively, approximating the low- and high-IFM limits applied experimentally by

Table 1 Elastic moduli and Poisson's ratios of component tissues (Simon et al. 2011)

	Elastic modulus (MPa)	Poisson's ratio
Cortical bone	10,000	0.36
Woven bone	4000	0.36
Cartilage	200	0.45
Granulation tissue	3	0.3

Claes et al. (1997). Simulations of healing under each fixation stiffness were run for a period representing 12 weeks post-injury. To test the proposed inverse dynamisation protocol, further simulations were conducted with stiffness increasing from 690 to 6250 N/mm at a time-point between one and 6 weeks.

Abaqus/standard (version 6.13-3, Dessault Systèmes Simulia Corp., Providence, RI, USA) was used for all finite element analyses. The algorithm governing tissue changes within the callus was implemented within the UMAT and URDFIL user subroutines. Solution-dependent state variables were used to track the volume fractions of each tissue type and vascularity. The elastic modulus, E, and Poisson's ratio, ν, were calculated from the state variables, according to Wehner et al. (2014):

$$E = E_{\text{Gran}} + (E_{\text{Cart}} - E_{\text{Gran}}) \cdot c_{\text{Cart}^3} + (E_{\text{Bone}} - E_{\text{Gran}}) \cdot c_{\text{Bone}^3}$$

$$\nu = \nu_{\text{Gran}} \cdot c_{\text{Gran}} + \nu_{\text{Cart}} \cdot c_{\text{Cart}} + \nu_{\text{Bone}} \cdot c_{\text{Bone}}$$

where c_i represents the volume fraction of tissue i, and "Gran", "Cart" and "Bone" subscripts denote undifferentiated granulation tissue, cartilage and woven bone respectively. Cortical bone was treated as non-changeable (E = 10 GPa, $\nu = 0.36$). The elastic moduli and Poisson's ratios corresponding to each component tissue were taken from Simon et al. (2011) and are shown in Table 1.

The mechano-biological scheme followed that reported by Simon et al. (2011), wherein tissue changes are determined by deviatoric and dilatational strains, and the composition of each element and its neighbours. This was derived from the regulatory scheme proposed originally by Claes and Heigele (1999), and reported in an iterative model using fuzzy logic by Shefelbine et al. (2005). Our implementation was verified by comparing results, using a similar sheep metatarsal geometry, to those reported by Simon et al. (2011). To complete the implementation and match results to those reported, details were incorporated from additional descriptions of the model (Chen et al. 2009; Niemeyer 2013; Shefelbine et al. 2005).

The rules governing tissue changes are outlined in Table 2. The corresponding fuzzy logic membership functions for each parameter and output (tissue change) were implemented, to the best of our knowledge, as by Simon et al. (2011).

To minimise the effect of different mesh densities on growth rates, changes in bone and perfusion fractions (which depend on fractions in adjacent elements) were scaled relative to element size (Simon et al. 2011), using a reference length of 0.22 mm. This corresponds to the estimated bony callus growth rate of 0.22 mm/day (Simon et al. 2011).

It was assumed that even a carefully conducted osteotomy would cause localised disruption to the blood supply. Therefore, we assumed that the cortex was initially avascular up to 1 mm from the fracture. Vascular boundary conditions were 30 % at the periphery of the periosteal callus zone and 100 % in the undamaged cortical bone; medullary perfusion was assumed to be restored after 10 days, also implemented as a 30 % boundary condition on the endosteal callus (Simon et al. 2011).

The simulations proceeded in steps representing 1 day, which provided adequate numerical stability and sufficient resolution for the mesh size and the maximum bone/vascular growth rate. At the end of each simulated week, the reaction force across the mid-plane of the fracture was output, along with the axial displacement of the fractured edge of the bone (i.e., half the IFM). The reaction force divided by the IFM gave an estimate of the axial stiffness of the callus. By plotting each state variable, the predicted tissue distributions could be monitored over time.

3 Results

According to the model, healing progressed fastest with the more rigid fixation (Fig. 2). The lower interfragmentary strain facilitated immediate chondrogenesis in and near the fracture gap, which calcified and ossified as soon as the vasculature grew into the region (see also Figure S1). Bridging of the gap was complete within 5 weeks, progressing from both the inner and outer surfaces of the cortex.

Under flexible fixation, the high strains within and adjacent to the fracture gap prevented chondrogenesis, which was concentrated adjacent to this zone (periosteally and endosteally), stimulated by moderate compressive dilatational strains (Fig. 2). The high gap strains also limited the progress of revascularisation, and directed periosteal bone growth outward, around the high-strain region. Once the advancing bone front connected with regions of more dense cartilage (in the fourth week), the strains in and near the gap were reduced to levels permitting chondrogenesis and endochondral ossification and, thereby, bridging. Endosteal bone growth was limited until bridging commenced.

Sustained bone growth, leading to higher densities of bone, was concentrated towards the periphery of the cal-

Table 2 Outline of mechano-biological rules governing tissue changes in the fracture callus, as used by Simon et al. (2011)

Deviatoric strain	Dilatational strain	Cartilage fraction	Bone fraction	Vascular fraction	Maximum neighbouring bone fraction	Maximum neighbouring vascular fraction	Result (fuzzy Output)
∼0	> −Medium	–	–	Low	–	Not low	Perfusion ↑
Low				Medium			
				High			
Low	±Low	Low		High	High	–	Woven bone ↑
Not destructive	−Medium	–	–	–	–	–	Cartilage ↑
	−Low						
Not destructive	−Medium	Not low	–	–	Not low	–	Cartilage ↓
	−Low						Woven bone ↑
	∼0						
	+Low						
∼0	±Low	Low	High	Not low	High	–	Cartilage ↓
Low							Woven bone ↑
Destructive							Cartilage ↓
	±Destructive	–	–	–	–	–	Woven bone ↓
							Perfusion ↓
–	Not ±Destructive	–	–	–	–	–	No change

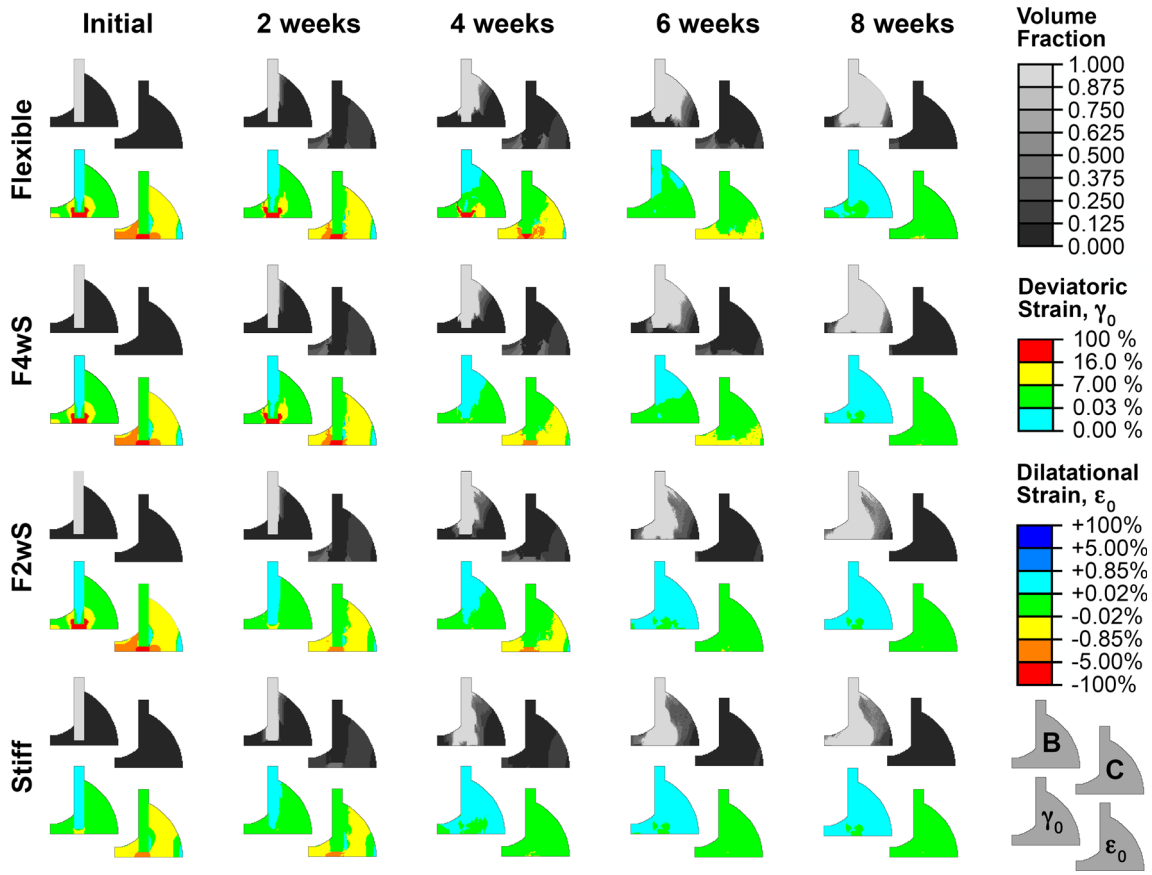

Fig. 2 Progression of healing under flexible fixation, inverse dynamisation and stiff fixation, as predicted by the mechano-biological scheme of Simon et al. (2011). The development of the callus tissues is shown at fortnightly intervals, by bone (*B, top left*) and cartilage (*C, top right*) volume fractions, along with the corresponding deviatoric (γ_0, *bottom left*) and dilatational (ε_0, *bottom right*) strains under load. The inverse dynamisation cases shown were supported by low fixation stiffness for the first two (F2wS) and four (F4wS) weeks, after which stiff fixation was maintained. Rapid cartilaginous bridging of the inter-cortical gap is evident after the stiffer fixation is applied, regardless of time-point. Calcification and ossification of the cartilage occur rapidly, allowing bony bridging to proceed from both periosteal and endosteal surfaces simultaneously. Endochondral bridging occurs more slowly, and commences more peripherally, under flexible fixation

lus under flexible fixation, and closer to the fracture under stiff fixation. The larger IFM thus corresponded to a larger volume of mature bony callus, prior to bridging. However, this did not confer a greater stiffness than the smaller callus volume produced under stiff fixation (Fig. 3); the stiffness only began to increase substantially under flexible fixation once the bone growth front connected with the cartilaginous region (4 weeks). By 12 weeks, little difference was apparent in callus sizes, as bone growth continued after bridging. This was consistent with similar final stiffness values under all conditions.

Increasing the fixation stiffness at a discrete time-point (i.e. inverse dynamisation) immediately reduced strains in the fracture gap to a pro-chondrogenic level. This allowed bridging to occur via the same chiefly endochondral mechanism, and over a similar timeframe, as in the case of constant stiff fixation. At no time-point did changing the fixation stiffness produce a superior result to stiff fixation alone. Increasing the stiffness after 4 weeks or more had little effect on healing rates or patterns, as the continuity between bony and cartilaginous regions provided increased stability, regardless.

4 Discussion

Inverse dynamisation, in which fixation stiffness begins low and is later increased for the consolidation phase, has been proposed as a means to produce faster, more reliable healing of diaphyseal bone fractures (Epari et al. 2013). In this study, we applied a published mechano-biological algorithm for predicting the course of fracture healing (Claes and Heigele 1999; Simon et al. 2011) to test this scenario against healing with constant low- and high-stiffness fixation. Using a model based on a sheep tibial osteotomy, the algorithm predicted the fastest, most direct healing under high fixation stiffness, and the slowest healing under constant low-stiffness fixation. The

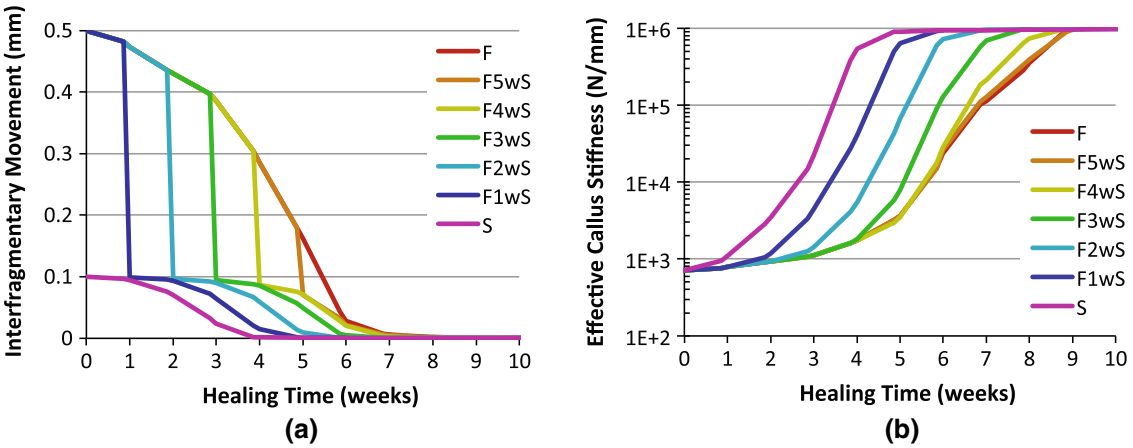

Fig. 3 Interfragmentary movement (**a**) and callus axial stiffness (**b**) over 10 weeks of the healing simulation, for stiff (*magenta*) and flexible (*red*) fixation and inverse dynamisation cases, with stiffness increased at time-points ranging from one (F1wS) to five (F5wS) weeks. The stiffness shown does not include that of the fixator, and both graphs show results for the half-section model geometry depicted in Fig. 1 (i.e. actual IFM is double that shown, and stiffness half). Irrespective of its timing, stiff fixation allows the callus stiffness to increase rapidly to a moderate level, corresponding to cartilage formation, followed immediately by further stiffening by calcification and endochondral ossification (refer to Fig. 2). The increasing callus size under flexible fixation is slow to affect stiffness, which increases rapidly only when the interfragmentary movement drops to a level similar to that under rigid fixation. This corresponds to continuity being established between cartilaginous and bony regions of the callus

model predicted no advantage in using inverse dynamisation, relative to maintaining the more rigid fixation throughout the healing process. The stiffness of the callus produced under flexible fixation never exceeded that produced under stiff fixation. The model did, however, predict that fracture consolidation could proceed rapidly after increasing the stiffness of an initially flexible fixation.

The present results are consistent with previous computational studies that predicted fastest healing under minimal mechanical stimulation (Chen et al. 2009; García-Aznar et al. 2007; Geris et al. 2010; Gómez-Benito et al. 2005, 2006; Isaksson et al. 2008; Kuiper et al. 2000; Lacroix and Prendergast 2002a, b; Simon et al. 2011; Wehner et al. 2010, 2012, 2014). In a related study, Kuiper et al. (2000) also found no advantage in a higher initial IFM, compared to a sustained low level of IFM, despite its stimulation of callus growth. Their finding that 25 % interfragmentary strain was more inhibitory than higher or lower magnitudes suggests that better healing outcomes may be possible for inverse dynamisation than presented here, but neither this nor the present study offer evidence that inverse dynamisation would result in faster healing than constant stiff fixation.

In all scenarios tested, the fracture gap was rapidly bridged by cartilage when IFM was below 0.1 mm (approximately 7 % interfragmentary strain). This strain limit was applied immediately by the stiffer fixation, but was not achieved by the callus until the sixth week of flexible fixation healing. Because this alone provided both a direct tissue pathway and the further reduction in strain required for endochondral ossification to progress, there was no advantage conferred by a larger callus. Furthermore, because the tissue change rates were constant and independent of mechanical conditions (within the given ranges), this consolidation proceeded over a similar timeframe for all cases, limited only slightly by the rate of gap vascularisation (see Figs. 2 and S1). Hence, although it is possible that a minimum stimulation is required to avoid atrophic non-union (Bailón-Plaza and van der Meulen 2003), the near-direct healing path facilitated by the stiff fixation in our simulations suggest that little further enhancement could be achieved.

As apparent in the results of the original model (Simon et al. 2011), the broad set of permissive mechanical conditions resulted in widespread early chondrogenesis, with subsequent cartilage deposition closer to the fracture. The cartilage in the peripheral callus confers little stiffness until it is mechanically continuous with the bony callus. This appears critical in the failure of the greater callus size stimulated by early high IFM to increase callus stiffness, as required by reverse dynamisation. Conversely, in low-IFM cases, cartilage in the gap provides this mechanical continuity, reducing strain to permit ossification. Because the regulatory scheme does not include resorption under very low levels of mechanical stimulus (see Shefelbine et al. 2005), and allows cartilage calcification under minimal strain, the widespread deposition of cartilage also facilitates the continued growth of bony callus after bridging of the fracture. This in turn contributes to the similar final (12-week) callus stiffness values across all models.

This study examined axial loading only, with the implicit assumption of high shear fixation stiffness. With adequate

material properties, a larger callus may confer a greater advantage in terms of bending stiffness. Based on this criterion, a computational study determined that a moderate axial and high shear stiffness are optimal (Steiner et al. 2014b). A three-dimensional model, incorporating shear and bending, may thus be more sensitive to the effects of inverse dynamisation on protecting the healing fracture from disruptive loading events.

In this study, we chose to implement a model based on an established regulatory scheme. We focused on the experimentally derived mechano-biological framework of Claes and Heigele (1999), emulating the iterative model of Simon et al. (2011). Although typically insufficient information is available to exactly replicate the fracture healing simulations published to date, combining additional information (Chen et al. 2009; Niemeyer 2013; Shefelbine et al. 2005; Wehner et al. 2010) with a series of trials provided similar results for a sheep metatarsal model to those published (Simon et al. 2011). The widespread early cartilage formation predicted by the present model (Simon et al. 2011), and the timing of chondrogenesis in the fracture gap, are not consistent with characterisations of typical histology (Vetter et al. 2010). Subsequent optimisation of the model (Steiner et al. 2013) appeared to predict more localised cartilage formation. Although possibly corresponding to a requirement for only medium (and not low) negative dilatational strains, the exact chondrogenesis rules were not specified, and insufficient detail precluded the use of this more recent model in the present study. Regardless, our aim was not to test the efficacy of any one model, but rather to predict the efficacy of a hypothetical treatment regime prior to experimental testing. A further aim is to encourage others to apply their specific models to this and other hypotheses, and to publish both the predicted results and subsequent comparison to experimental data.

The simulations presented are a first step in testing the principle of inverse dynamisation; nonetheless, the results of in vivo experimental testing are essential to complete the assessment of the methodology. Upon publication of this data, comparing them to separately published computational results provides a test of the models' predictive power with full transparency. By testing similar scenarios in computational and experimental models, the scope and relevance of histological and mechanical comparisons can be maximised. If the in vivo results agree that early flexible fixation and subsequently increasing stiffness confers no advantage, then the observations discussed above may help us to understand the reasons for the failure of the method. Conversely, should the experimental data contradict the present results, the comparisons will help in identifying improvements needed in the computational models, the mechano-regulation scheme and/or its implementation.

To our knowledge, this is the first time iterative computational models of fracture healing mechano-biology have been applied to predict the outcomes of a hypothetical treatment regime, ahead of experimental testing. We propose that the publication of hypotheses and their subsequent testing using computational models, prior to in vivo experimentation, can foster the ongoing refinement and validation of mechano-biological models, with increased transparency. We believe this to be a necessary step towards applying models with confidence in a clinically relevant context.

5 Disclosure

A key component of this study was that simulations were conducted blinded to experimental data. While Dr. Epari supervised both experimental and modelling projects, the model was coded and executed by Dr. Wilson, who was blinded to the experimental work. Although Dr. Epari was active in the conceptualisation, design and reporting of this work, he did not influence the interpretation of the models' results. Similarly Prof. Schütz contributed to project conceptualisation, clinical context and manuscript preparation, but was not directly involved in the simulation work.

Acknowledgements This work was assisted by a Discovery Project Grant (DP0988124) from the Australian Research Council. The computational work was facilitated by the High Performance Computing facility at QUT. Dr. Wilson would like to especially thank Mr Abdul Sharif and Dr. Lance Wilson for remote-access support. The authors acknowledge Dr. Gongfa Chen for his work in implementing early versions of the iterative model framework in Abaqus.

References

Ament C, Hofer EP (2000) A fuzzy logic model of fracture healing. J Biomech 33:961–968. doi:10.1016/S0021-9290(00)00049-X

Andreykiv A, van Keulen F, Prendergast PJ (2008) Simulation of fracture healing incorporating mechanoregulation of tissue differentiation and dispersal/proliferation of cells. Biomech Model Mechanobiol 7:443–461. doi:10.1007/s10237-007-0108-8

Bailón-Plaza A, van der Meulen MCH (2003) Beneficial effects of moderate, early loading and adverse effects of delayed or excessive loading on bone healing. J Biomech 36:1069–1077. doi:10.1016/S0021-9290(03)00117-9

Byrne DP, Lacroix D, Prendergast PJ (2011) Simulation of fracture healing in the tibia: mechanoregulation of cell activity using a lattice modeling approach. J Orthop Res 29:1496–1503. doi:10.1002/jor.21362

Checa S, Prendergast PJ, Duda GN (2011) Inter-species investigation of the mechano-regulation of bone healing: comparison of secondary bone healing in sheep and rat. J Biomech 44:1237–1245. doi:10.1016/j.jbiomech.2011.02.074

Chen G, Niemeyer F, Wehner T, Simon U, Schuetz MA, Pearcy MJ, Claes LE (2009) Simulation of the nutrient supply in fracture healing. J Biomech 42:2575–2583. doi:10.1016/j.jbiomech.2009.07.010

Claes L, Heigele CA (1999) Magnitudes of local stress and strain along bony surfaces predict the course and type of fracture healing. J Biomech 32:255–266. doi:10.1016/S0021-9290(98)00153-5

Claes L, Augat P, Suger G, Wilke HJ (1997) Influence of size and stability of the osteotomy gap on the success of fracture healing. J Orthop Res 15:577–584. doi:10.1002/jor.1100150414

Claes L, Wolf S, Augat P (2000) Mechanische Einflüsse auf die Callusheilung (mechanical influences on callus healing). Chirurg 71:989. doi:10.1007/s001040051172

Doblaré M, García JM, Gómez MJ (2004) Modelling bone tissue fracture and healing: a review. Eng Fract Mech 71:1809–1840

Einhorn TA (1998) The cell and molecular biology of fracture healing. Clin Orthop Relat Res 355:S7–S21

Epari DR, Schell H, Bail HJ, Duda GN (2006) Instability prolongs the chondral phase during bone healing in sheep. Bone 38:864–870. doi:10.1016/j.bone.2005.10.023

Epari DR, Wehner T, Ignatius A, Schuetz MA, Claes LE (2013) A case for optimising fracture healing through inverse dynamization. Med Hypotheses 81:225–227. doi:10.1016/j.mehy.2013.04.044

García-Aznar JM, Kuiper JH, Gómez-Benito MJ, Doblaré M, Richardson JB (2007) Computational simulation of fracture healing: influence of interfragmentary movement on the callus growth. J Biomech 40:1467–1476. doi:10.1016/j.jbiomech.2006.06.013

Geris L, Vander Sloten J, Van Oosterwyck H (2009) In silico biology of bone modelling and remodelling: regeneration. Philos Trans A Math Phys Eng Sci 367:2031–2053. doi:10.1098/rsta.2008.0293

Geris L, Sloten JV, Van Oosterwyck H (2010) Connecting biology and mechanics in fracture healing: an integrated mathematical modeling framework for the study of nonunions. Biomech Model Mechanobiol 9:713–724. doi:10.1007/s10237-010-0208-8

Gómez-Benito MJ, García-Aznar JM, Kuiper JH, Doblaré M (2005) Influence of fracture gap size on the pattern of long bone healing: a computational study. J Theor Biol 235:105–119. doi:10.1016/j.jtbi.2004.12.023

Gómez-Benito MJ, García-Aznar JM, Kuiper JH, Doblaré M (2006) A 3D computational simulation of fracture callus formation: influence of the stiffness of the external fixator. J Biomech Eng 128:290–299. doi:10.1115/1.2187045

Gómez-Benito MJ, González-Torres LA, Reina-Romo E, Grasa J, Seral B, García-Aznar JM (2011) Influence of high-frequency cyclical stimulation on the bone fracture-healing process: mathematical and experimental models. Philos Trans A Math Phys Eng Sci 369:4278–4294. doi:10.1098/rsta.2011.0153

González-Torres LA, Gómez-Benito MJ, Doblaré M, García-Aznar JM (2010) Influence of the frequency of the external mechanical stimulus on bone healing: a computational study. Med Eng Phys 32:363–371. doi:10.1016/j.medengphy.2010.01.010

Hayward LN, Morgan EF (2009) Assessment of a mechano-regulation theory of skeletal tissue differentiation in an in vivo model of mechanically induced cartilage formation. Biomech Model Mechanobiol 8:447–455. doi:10.1007/s10237-009-0148-3

Huiskes R, Van Driel WD, Prendergast PJ, Soballe K (1997) A biomechanical regulatory model for periprosthetic fibrous-tissue differentiation. J Mater Sci Mater Med 8:785–788

Isaksson H (2012) Recent advances in mechanobiological modeling of bone regeneration. Mech Res Commun 42:22–31. doi:10.1016/j.mechrescom.2011.11.006

Isaksson H, van Donkelaar CC, Huiskes R, Ito K (2006a) Corroboration of mechanoregulatory algorithms for tissue differentiation during fracture healing: comparison with in vivo results. J Orthop Res 24:898–907. doi:10.1002/jor.20118

Isaksson H, Wilson W, van Donkelaar CC, Huiskes R, Ito K (2006b) Comparison of biophysical stimuli for mechano-regulation of tissue differentiation during fracture healing. J Biomech 39:1507–1516. doi:10.1016/j.jbiomech.2005.01.037

Isaksson H, van Donkelaar CC, Huiskes R, Ito K (2008) A mechano-regulatory bone-healing model incorporating cell-phenotype specific activity. J Theor Biol 252:230–246. doi:10.1016/j.jtbi.2008.01.030

Isaksson H, van Donkelaar CC, Ito K (2009) Sensitivity of tissue differentiation and bone healing predictions to tissue properties. J Biomech 42:555–564. doi:10.1016/j.jbiomech.2009.01.001

Khayyeri H, Isaksson H, Prendergast PJ (2013) Corroboration of computational models for mechanoregulated stem cell differentiation. Comput Methods Biomech Biomed Engin. doi:10.1080/10255842.2013.774381

Kuiper JH, Richardson JB, Ashton BA (2000) Computer simulation to study the effect of fracture site movement on tissue formation and fracture stiffness restoration. In: European congress on computational methods in applied sciences and engineering (ECCOMAS), Barcelona, 11–14 Sept 2000

Lacroix D, Prendergast PJ (2002a) A mechano-regulation model for tissue differentiation during fracture healing: analysis of gap size and loading. J Biomech 35:1163–1171. doi:10.1016/S0021-9290(02)00086-6

Lacroix D, Prendergast PJ (2002b) Three-dimensional simulation of fracture repair in the human tibia. Comput Methods Biomech Biomed Engin 5:369–376. doi:10.1080/1025584021000025014

Lacroix D, Prendergast PJ, Li G, Marsh D (2002) Biomechanical model to simulate tissue differentiation and bone regeneration: application to fracture healing. Med Biol Eng Comput 40:14–21. doi:10.1007/BF02347690

McKibbin B (1978) The biology of fracture healing in long bones. J Bone Joint Surg Br 60–B:150–162

Niemeyer F (2013) Simulation of fracture healing applied to distraction osteogenesis. Dissertation, Universität Ulm

Peters A, Schell H, Bail HJ, Hannemann M, Schumann T, Duda GN, Lienau J (2010) Standard bone healing stages occur during delayed bone healing, albeit with a different temporal onset and spatial distribution of callus tissues. Histol Histopathol 25:1149–1162

Pivonka P, Dunstan CR (2012) Role of mathematical modeling in bone fracture healing. Bonekey Rep 1:221. doi:10.1038/bonekey.2012.221

Prendergast PJ, Huiskes R (1996) Finite element analysis of fibrous tissue morphogenesis—a study of the osteogenic index with a biphasic approach. Mech Compos Mater 32:144–150

Prendergast PJ, Huiskes R, Søballe K (1997) Biophysical stimuli on cells during tissue differentiation at implant interfaces. J Biomech 30:539–548. doi:10.1016/S0021-9290(96)00140-6

Repp F, Vetter A, Duda GN, Weinkamer R (2015) The connection between cellular mechanoregulation and tissue patterns during bone healing. Med Biol Eng Comput. doi:10.1007/s11517-015-1285-8

Shefelbine SJ, Augat P, Claes L, Simon U (2005) Trabecular bone fracture healing simulation with finite element analysis and fuzzy logic. J Biomech 38:2440–2450. doi:10.1016/j.jbiomech.2004.10.019

Simon U, Augat P, Utz M, Claes L (2011) A numerical model of the fracture healing process that describes tissue development and revascularisation. Comput Methods Biomech Biomed Engin 14:79–79. doi:10.1080/10255842.2010.49986

Steiner M, Claes L, Ignatius A, Niemeyer F, Simon U, Wehner T (2013) Prediction of fracture healing under axial loading, shear loading and bending is possible using distortional and dilatational strains as determining mechanical stimuli. J R Soc Interface 10. doi:10.1098/rsif.2013.0389

Steiner M, Claes L, Ignatius A, Simon U, Wehner T (2014a) Disadvantages of interfragmentary shear on fracture healing-mechanical insights through numerical simulation. J Orthop Res 32:865–872. doi:10.1002/jor.22617

Steiner M, Claes L, Ignatius A, Simon U, Wehner T (2014b) Numerical simulation of callus healing for optimization of fracture fixation stiffness. PloS One 9:e101370. doi:10.1371/journal.pone.0101370

Stürmer KM (1984) Histologische Befunde der Frakturheilung unter Fixateur externe und ihre klinische Bedeutung. Unfallchirurgie 10:110–122. doi:10.1007/BF02585799

van Driel WD, Huiskes HWJ, Prendergast PJ (1998) A regulatory model for tissue differentiation using poroelastic theory. In: Thimus J-F, Abousleiman Y, Cheng AH-D, Coussy O, Detournay E (eds) Biot conference on poromechanics, Louvain-la-Neuve, Belgium, 14–16 September 1998. Balkema, Rotterdam, pp 409–413

Vetter A, Epari DR, Seidel R, Schell H, Fratzl P, Duda GN, Weinkamer R (2010) Temporal tissue patterns in bone healing of sheep. J Orthop Res 28:1440–1447. doi:10.1002/jor.21175

Vetter A, Witt F, Sander O, Duda GN, Weinkamer R (2012) The spatio-temporal arrangement of different tissues during bone healing as a result of simple mechanobiological rules. Biomech Model Mechanobiol 11:147–160. doi:10.1007/s10237-011-0299-x

Wehner T, Claes L, Niemeyer F, Nolte D, Simon U (2010) Influence of the fixation stability on the healing time—a numerical study of a patient-specific fracture healing process. Clin Biomech (Bristol, Avon) 25:606–612. doi:10.1016/j.clinbiomech.2010.03.003

Wehner T, Claes L, Ignatius A, Simon U (2012) Optimization of intramedullary nailing by numerical simulation of fracture healing. J Orthop Res 30:569–573. doi:10.1002/jor.21568

Wehner T, Steiner M, Ignatius A, Claes L (2014) Prediction of the time course of callus stiffness as a function of mechanical parameters in experimental rat fracture healing studies-a numerical study. PloS One 9:e115695. doi:10.1371/journal.pone.0115695

Witt F, Petersen A, Seidel R, Vetter A, Weinkamer R, Duda GN (2011) Combined in vivo/in silico study of mechanobiological mechanisms during endochondral ossification in bone healing. Ann Biomed Eng 39:2531–2541. doi:10.1007/s10439-011-0338-x